Detection of low density lipoprotein particle fusion by proton nuclear magnetic resonance spectroscopy

Mika Ala-Korpela,[1,*] Markku O. Pentikäinen,* Ari Korhonen,[†] Tiia Hevonoja,* Juhani Lounila,[†] and Petri T. Kovanen*

Wihuri Research Institute,* Kalliolinnantie 4, FIN-00140 Helsinki, Finland, and Department of Physical Sciences,[†] NMR Research Group, University of Oulu, P. O. Box 333, FIN-90571 Oulu, Finland

Abstract **Recent evidence suggests that fusion of low density lipoprotein (LDL) particles is a key process in the initial accumulation of lipid in the arterial intima. In order to gain a better understanding of this early event in the development of atherosclerosis, it would thus be necessary to characterize the process of LDL fusion in detail. Such studies, however, pose severe methodological difficulties, such as differentiation of particle fusion from aggregation. In this paper we describe the use of novel methodology, based on ^{1}H NMR spectroscopy, to study lipoprotein particle fusion. To test the methodology, we chose proteolytic fusion of LDL particles, an in vitro model that has been well characterized in our laboratory. The spectroscopic data suggested that proteolysis of LDL with α-chymotrypsin induced slow initiation of fusion, which was followed by particle fusion at an increased rate. Moreover, ^{1}H NMR spectroscopic data on different kinds of LDL interactions, for example, when LDL formed aggregates with antibodies against human apolipoprotein B-100, were obtained and compared with the electron microscopic characteristics of these preparations. An important finding was that limited aggregation of LDL particles did not disturb the ^{1}H NMR spectroscopic parameters used for the detection of particle fusion and preserved the physicochemical information on the particles. The ^{1}H NMR methodology developed is sensitive to and specific for low density lipoprotein (LDL) fusion and may also allow for studies of the fate of LDL particles in other in vitro preparations that mimic the arterial interactions in vivo.—**Ala-Korpela, M., M. O. Pentikäinen. A. Korhonen, T. Hevonoja, J. Lounila, and P. T. Kovanen. **Detection of low density lipoprotein particle fusion by proton nuclear magnetic resonance spectroscopy. *J. Lipid Res.* 1998.** 39: **1705–1712.**

Supplementary key words fusion • lipid accumulation • low density lipoprotein • nuclear magnetic resonance spectroscopy • proteolysis

The initial morphological characteristic of both human (1, 2) and experimental (3) atherosclerosis is accumulation of lipid droplets (~100–400 nm in diameter) in the subendothelial extracellular space of the arterial intima prior to recruitment of monocytes and formation of foam cells. The lipid droplets are presumed to originate from low density lipoprotein (LDL) particles (average diameter ~22 nm) that enter the subendothelial space (3–5). To form such lipid droplets, LDL particles have to undergo fusion (6, 7). However, prolonged incubation, even in the presence of arterial proteoglycans, does not lead to significant fusion of LDL particles (8). Therefore, it is evident that, before they can undergo fusion, the LDL particles have to be modified. The modifications causing LDL fusion in vivo are not known, but several modifications are known to trigger LDL fusion in vitro. These modifications include proteolysis of the apolipoprotein B-100 (apoB-100) component at the surface of the LDL particles (9–12) and treatment of the surface phospholipids with sphingomyelinase (13, 14) or phospholipase A_2 (15). In addition, vortexing (16, 17), oxidation (18), or combined treatment with trypsin and cholesteryl esterase (19) can labilize LDL particles sufficiently to allow particle fusion. In contrast, other modifications, e.g., glycosylation or treatment with malondialdehyde (20), do not trigger LDL fusion even though they lead to aggregation of the particles.

Studies of lipoprotein fusion have suffered from methodological difficulties. The biochemical methods that are available for particle size analysis, e.g., gel filtration chromatography, molecular sieving electrophoresis, and analytical ultracentrifugation, cannot differentiate fusion from aggregation. Negative staining electron microscopy is suitable for analyzing the size of native LDL particles, but suffers from artificial aggregation of particles during sample preparation and from inability to detect characteristics of the individual particles in aggregates. On the other hand, thin-section electron microscopy of embedded LDL particles is suitable for analyzing the morphology of the enlarged particles even in aggregates. However, both electron microscopy methods suffer from poor guarantee of the representability of the samples. As part of our

Abbreviations: anti-apoB-100, antibody to human apolipoprotein B-100; D_2O, deuterium oxide; FID, free induction decay; LDL, low density lipoprotein; NMR, nuclear magnetic resonance; TCA, trichloroacetic acid; TSP, sodium 3-trimethylsilyl[2,2,3,3-D_4] propionate.

[1]To whom correspondence should be addressed.

efforts to understand lipoprotein particle fusion, we have recently developed a fusion assay that is based on fluorescent resonance energy transfer (8). This is able to detect LDL fusion even in LDL aggregates, but it requires preparation of two populations of fluorescently labeled LDL particles and can neither detect small changes in particle size nor quantify the changes.

Proton nuclear magnetic resonance (^{1}H NMR) spectroscopy has proved to be a powerful tool for plasma and lipoprotein analysis (21–31). Because the protons detectable with NMR are part of the natural molecular structure of the particles, there is no need for lipid labeling or particle modification when using ^{1}H NMR spectroscopy. It can thus be applied for noninvasive detection of lipids in native lipoprotein particles and their mixtures (24–31). The great abundance of protons in lipoprotein samples also makes continuous follow-up of processes possible without interference. Moreover, information can be obtained about the physico-chemical characteristics of the particles. Importantly, experimental findings have shown that, with a decrease in the lipoprotein particle size, the ^{1}H NMR spectroscopy resonances from the hydrocarbon chains of the lipoprotein lipids shift systematically to lower frequencies (21–24, 30–32). The basis of this particle size-dependent frequency behavior has recently been explained theoretically by a simple physical model for the lipoprotein particle structure (33). The particle model, via magnetic field equations, leads to a formulation that links the experimentally observed frequency shifts with the size of the particles and thus provides a practical means for detailed studies of lipoprotein particle fusion by ^{1}H NMR spectroscopy.

We have previously studied the proteolytic modification of LDL in vitro as a model of LDL fusion in the arterial intima (8–12). We have found that degradation of apoB-100 with loss of fragments of apoB-100 leads to fusion of the LDL particles (10). In this paper we demonstrate the strength of the ^{1}H NMR methodology with results for proteolytic fusion of LDL and discuss the methodological details of how lipoprotein particle fusion can be studied by ^{1}H NMR.

EXPERIMENTAL PROCEDURES

Materials

Dextran sulfate sodium salt (Mw 500,000) and PD-10 columns were from Pharmacia, and α-chymotrypsin (from bovine pancreas), deuterium oxide (D_2O), and heparin were from Sigma. Antibodies against human apolipoprotein B-100 (anti-apoB-100), from sheep and goat, were from Boehringer Mannheim and from Biodesign International, respectively. Bio-Gel A-5m was from Bio-Rad, NuSieve GTG low-melting-point agarose from FMC Corp. BioProducts, Dulbecco's phosphate-buffered saline from Life Technologies, Inc., [1,2-^{3}H]cholesteryl linoleate from Amersham, Celite 545 (acid washed) from Fluka, and [^{3}H]heparin from DuPont NEN.

Isolation and modifications of LDL

Seven preparations of human LDL (d 1.019–1.050 g/ml) were isolated from unpooled plasma of four apparently healthy laboratory persons by sequential ultracentrifugation (34). The isolated LDL was dialyzed extensively against buffer A (150 mm NaCl, 1 mm EDTA, pH 7.4), filtered through a 0.22-μm filter, fractionated, and stored at 4°C. Each experiment was carried out using a single LDL preparation. For some experiments, LDL was labeled with [^{3}H] cholesteryl linoleate as described previously (10). The NMR measurements were carried out in buffer B (137 mm NaCl, 2.7 mm KCl, 10 μm Na_2EDTA, 10 mm phosphate, pD 7.0 in D_2O) (29) unless otherwise indicated. To change the buffer, LDL was gel-filtered twice through PD-10 columns equilibrated and eluted with buffer B. The amounts and concentrations of LDL are expressed in terms of protein, which was determined by the procedure of Lowry et al. (35) with bovine serum albumin as standard.

LDL was proteolyzed by incubating LDL (1 mg/ml) with α-chymotrypsin (0.1 mg/ml) in buffer B for the indicated times at 37°C (10, 20). LDL–sheep anti-apoB-100 complexes were prepared by incubating 1 mg of LDL with 300 μl of sheep anti-apoB-100 in 1 ml of buffer A for 20 min at room temperature. The complexes formed were sedimented by centrifugation (20,000 *g* for 5 min), washed once with 1 ml of buffer B, and dissolved in 600 μl of buffer B. LDL–goat anti-apoB-100 complexes were prepared by incubating 250 μl of goat anti-apoB-100 with 500 μg of LDL in 500 μl of Dulbecco's phosphate-buffered saline supplemented with 10 μm Na_2EDTA for 15 min at 37°C. These complexes did not sediment on centrifugation at 20,000 *g* for 10 min, but in control experiments 54% and 53% of radiolabeled LDL were in structures larger than native LDL in size-exclusion chromatography on a Bio-Gel A-5m (1 × 60 cm) column and in rate zonal flotation (experiments were performed as described in ref. 20), respectively. LDL–dextran sulfate complexes were prepared by incubating LDL (1 mg/ml) with dextran sulfate (0.1 mg/ml) in buffer B for 20 min at room temperature. Preliminary experiments showed that, under these conditions, over 90% of the LDL can be precipitated by centrifugation at 20,000 *g* for 10 min. LDL–heparin complexes were prepared by incubating LDL (1 mg/ml) with heparin (0.1 mg/ml) in buffer B for 20 min at room temperature. LDL was found to bind heparin in a gel mobility shift assay (36) (with an apparent affinity constant of approximately 2 μm^{-1} LDL) but we were unable to demonstrate any aggregation of LDL by heparin when analyzed with gel filtration chromatography or centrifugation at 20,000 *g*.

Electron microscopy

Samples were processed for thin-section electron microscopy exactly as described previously (8) and viewed in a Jeol JEM-1200EX transmission electron microscope at the Institute of Biotechnology, Electron Microscopy, University of Helsinki (Helsinki, Finland).

^{1}H NMR spectroscopy

The ^{1}H NMR data were acquired at 37°C on a Bruker DRX 500 MHz spectrometer at the NMR laboratory, University of Oulu (Oulu, Finland). A sealed coaxial insert (outer diameter 2 mm) containing an external standard, sodium 3-trimethylsilyl[2,2,3,3-D_4] propionate (TSP) (8 mmol/l) and $MnSO_4$ (0.6 mmol/l) in 99.8% D_2O, was used with every sample (0.465 ml) placed in a 5-mm NMR tube (24). In each experiment 64 FID signals of 64 k data points were accumulated using a pulse repetition time of 6.6 s and 90° pulses. The spectral widths were 6.25 kHz. In the case of the LDL–goat anti-apoB-100 complex and the corresponding native LDL control, the intense water peak was suppressed by the SHAKA-180° pulse sequence (37). LDL and LDL plus α-chymotrypsin samples were incubated in the magnet for up to 48 h and the data were recorded every 10 to 60 min. Three different experiments for α-chymotrypsin-induced fusion of LDL particles were carried out leading to follow-up data sets, each consisting of from 48 to 286 individual spectra.

The measured FIDs were Fourier transformed without apodization to the frequency domain spectra, in which the cho-

lesterol backbone –C(18)$\underline{H}_3$ (at around ~0.6 ppm), the terminal methyl –C$\underline{H}_3$ (~0.8 ppm) and the methylene =CH–C$\underline{H}_2$–CH= (~2.7 ppm) resonances were subjected to lineshape fitting analysis to accurately resolve the frequencies of the resonances. The –C(18)$\underline{H}_3$ and –C$\underline{H}_3$ resonances were fitted with one and the =CH–C$\underline{H}_2$–CH= resonance with three Lorentzians. A linear baseline and a phase parameter were also estimated for each resonance region analyzed. Program FITPLA[C] was applied (23, 24, 30–32). At the concentrations and under the experimental conditions used, α-chymotrypsin gave a hardly detectable broad signal over the frequency range studied and thus did not disturb the lineshape fitting analysis in the narrow resonance regions (data not shown).

THEORETICAL BASIS

A physical model has recently been developed for lipoprotein particle structure to explain why the ^{1}H NMR resonances from the lipoprotein lipids shift systematically to lower frequencies with a decrease in particle size (33). The explanation of this phenomenon turned out to be the anisotropy of the magnetic susceptibility due to orientation of the surface monolayer of the lipoprotein particles. When the magnetic field equations for a spherical particle with an isotropic core and a radially oriented surface were solved, a simple equation linking the frequency of the i^{th} NMR line, ν_i, and the lipoprotein particle radius, R, was obtained (in SI units):

$$\nu_i(R) = \nu_i^0 + \frac{2}{3}\,\nu_0 \Delta\chi \ln\frac{R}{R-\Delta}. \qquad \textit{Eq. 1}$$

Here ν_i^0 is the asymptotic value of ν_i at limit $R \rightarrow \infty$, ν_o is the operating frequency of the spectrometer, $\Delta\chi$ is the anisotropy of the magnetic volume susceptibility of the particle surface, and Δ is the thickness of the surface. As the frequency ν_i is now an explicit function of the radius R, this model leads in a natural way to systematic dependence of the frequency observable with NMR on the size of the lipoprotein particles.

The above theoretical formulation provides a means for dynamic follow-up of lipoprotein particle fusion and also for distinguishing fusion from aggregation of the particles. According to Eq. 1, an increase in particle size causes a shift toward higher resonance frequencies and a decrease in size toward lower frequencies, provided that $\Delta\chi$ is negative (as it is in simple micelles making up lyotropic crystals (33)). Particle aggregation, which brings the surface monolayers of different lipoprotein particles into contact but does not unite them and thus does not change the size of the individual particles, should not cause any change in the frequency of the lipid resonances. In contrast, molecular mobility and overall tumbling of the resonating molecules affect the visibility and shape of the individual resonances. Thus, interactions that restrict mobility within the sample can lead to characteristic changes not only at specific resonance frequencies but also in the whole spectral appearance. Global broadening (or disappearance) of resonances will thus be a sign of aggregation or complex formation in the sample but will contrast with the frequency changes of all the lipoprotein lipid fatty acid resonances predicted by Eq. 1 in the case of particle fusion.

Here, it should be pointed out that, in the current application of the physical lipoprotein particle model, the thickness, Δ, and the anisotropy of the magnetic susceptibility, $\Delta\chi$, of the surface monolayer are assumed to be constant for particles of different sizes. Even though this approximation, with values of 2.0 nm for Δ and −0.223 ppm for $\Delta\chi$ (in SI units), has been applied successfully to modeling the size-dependent frequency behavior throughout the different lipoprotein categories, i.e., very low, intermediate, low, and high density lipoprotein particles (33), this approximation may not strictly hold during the process of particle fusion which can lead to remarkable changes in surface composition and structure. The extent to which these structural changes may affect the values of Δ and $\Delta\chi$ is not currently known, and thus these seemingly unavoidable approximations and their possible effects have to be borne in mind when making quantitative comparisons with other methods. Comparison with electron microscopy, however, suggests that the effects are minor (see Results and Discussion section below). Thus, in addition to clear phenomenological information on lipoprotein particle interactions, including specific detection of fusion, this methodology will also allow quantitative assessment of the changes in lipoprotein particle size.

RESULTS AND DISCUSSION

In this work, LDL was proteolyzed with α-chymotrypsin under conditions similar to those used previously (8, 10, 20). Under these conditions, intact apoB-100 disappears within 6 h and 60% of the radiolabeled apoB-100 is found as TCA-soluble fragments (<5,000 kDa) at 24 h. **Figure 1** shows the frequency behavior of the cholesterol backbone –C(18)$\underline{H}_3$, the terminal methyl –C$\underline{H}_3$ and the methylene =CH–C$\underline{H}_2$–CH= ^{1}H NMR resonances in an α-chymotrypsin-treated LDL sample followed within the NMR spectrometer. It can be clearly seen that all these lipid resonances, which provide a representative sample of the lipid environments in the particle, shifted toward higher frequencies as a function of time. When LDL was incubated in the absence of α-chymotrypsin, no such changes were observed. According to the theoretical formulation (Eq. 1), the shift toward higher frequencies is an indication of increases in the size of individual particles in the sample. This finding is in good accord with the known effects of α-chymotrypsin on LDL, i.e., particle fusion (20). It is notable that when LDL was incubated with α-chymotrypsin, all the lipid resonances, though originating from different chemical environments, underwent very similar changes in frequency. This kind of homogeneous response of protons in different chemical environments is due to a general physical phenomenon, the anisotropy of the magnetic susceptibility ($\Delta\chi$ in Eq. 1) of the oriented surface monolayer of the LDL particles (33). Thus, the lipoprotein particle structure itself gives rise to an overall magnetic disturbance, which is independent of the local chemical environment of the individual classes of resonating nuclei.

As the proteolytic degradation of LDL apoB-100 was accomplished within the spectrometer, it was convenient to follow the kinetics of the α-chymotrypsin-induced changes on the LDL particles. Three different experiments were performed in which LDL was incubated for up to 48 h in the presence of α-chymotrypsin, the time resolution of the ^{1}H NMR measurements varying from 10 to 60 min. All measurements gave consistent frequency changes for the various lipid resonances of the LDL particles, a result which, according to the physical model and Eq. 1, suggests similar and reproducible kinetics of LDL particle fu-

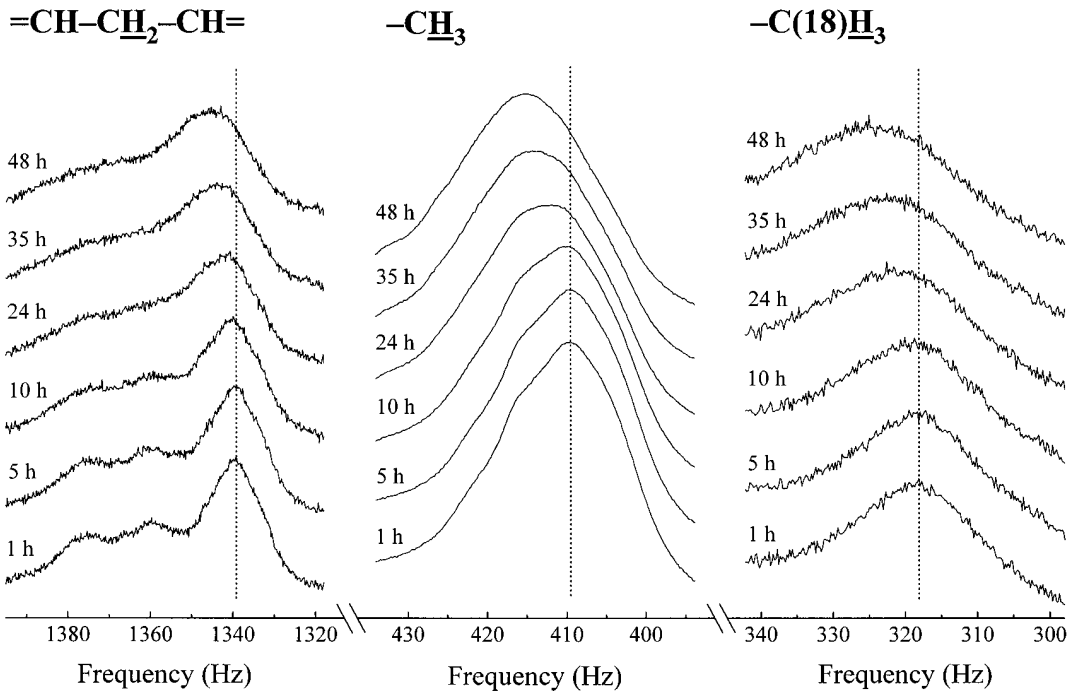

Fig. 1. Resonances of the cholesterol backbone –C(18)$\underline{H}_3$, the terminal methyl –C$\underline{H}_3$, and the methylene =CH–C$\underline{H}_2$–CH= in the ^{1}H NMR spectra of an α-chymotrypsin-treated LDL sample at some indicated time points. The dotted lines at the resonance positions are drawn to illustrate the systematic shift of each resonance position toward a higher frequency as a function of time. The spectra are referenced to the TSP resonance at 0.0 Hz.

sion resulting from the proteolytic modification induced by α-chymotrypsin. **Figure 2** (panels A–C) illustrates the changes in the size of the LDL particles, as calculated from the frequency shifts of the three distinct lipid resonances analyzed using Eq. 1, in one typical set of measurements for LDL incubated in the presence or absence of α-chymotrypsin. Very similar LDL particle size behavior was observed in all these lipid resonances, which accords with theoretical expectations (33). As the methylene =CH–C$\underline{H}_2$–CH= and the cholesterol backbone –C(18)$\underline{H}_3$ resonances have a lower signal-to-noise ratio than the terminal methyl –C$\underline{H}_3$ resonance, the LDL diameters derived from their frequency shifts are slightly more scattered than those from the –C$\underline{H}_3$ resonance. When native LDL was incubated alone (in the absence of α-chymotrypsin), all the resonance frequencies were constant over the 48-h period (standard deviation less than 1% of the mean when calculated from the –C$\underline{H}_3$ resonance). This indicates that native LDL particles, at the relatively high concentration used (1 mg/ml apoB-100), showed no tendency to fuse at body temperature.

Figure 2 shows a progressive increase in LDL particle size when LDL was incubated in the presence of α-chymotrypsin. The average size of the LDL particles as a function of time follows an exponential behavior quite closely, indicating continuous enhancement in the rate of increase in particle size; the average percentage increase in the LDL particle diameter is also illustrated in Fig. 2 (panel D) in another experiment (with 10 min time resolution). Behavior of this kind suggests that a certain degree of proteolytic modification is required before the events leading to fusion between the LDL particles start to take place. This is consistent with recent results showing that release of apoB-100 peptides from the LDL surface is, in fact, a prerequisite for fusion; proteolytic treatment of LDL, which only cleaved apoB-100 into specific fragments that remained bound to the particle, did not trigger particle fusion (10). This result is not unexpected, as continuous particle fusion leads to an increased number of larger particles and thus also to an increased probability that fusion will occur between the larger particles. As fusion progresses, the increase in particle size tends to be much more pronounced than in the beginning of proteolytic fusion, when the fusion events are between native or almost native-sized particles, and therefore lead only to a minor increase in the size of the fusion product. The continuous release of apoB-100 peptides from the particle surfaces, and the concomitant loosening of the surface integrity, may also in part tend to enhance the rate of particle fusion. In conclusion, the current results suggest that proteolytic modification of LDL particles, as induced by α-chymotrypsin, leads to progressive particle fusion which generates LDL-derived particles of increased size at an increasing rate.

Previous analysis of proteolyzed LDL particles from our laboratory allows for some comparison to be made between the current ^{1}H NMR results and results obtained with several other methods (8, 10, 20). Size-exclusion chromatography has clearly shown that proteolysis of LDL with α-chymotrypsin produces LDL derived structures with increased size, but this method does not allow determination of the particle size beyond the exclusion limit of the column and cannot differentiate fusion from aggrega-

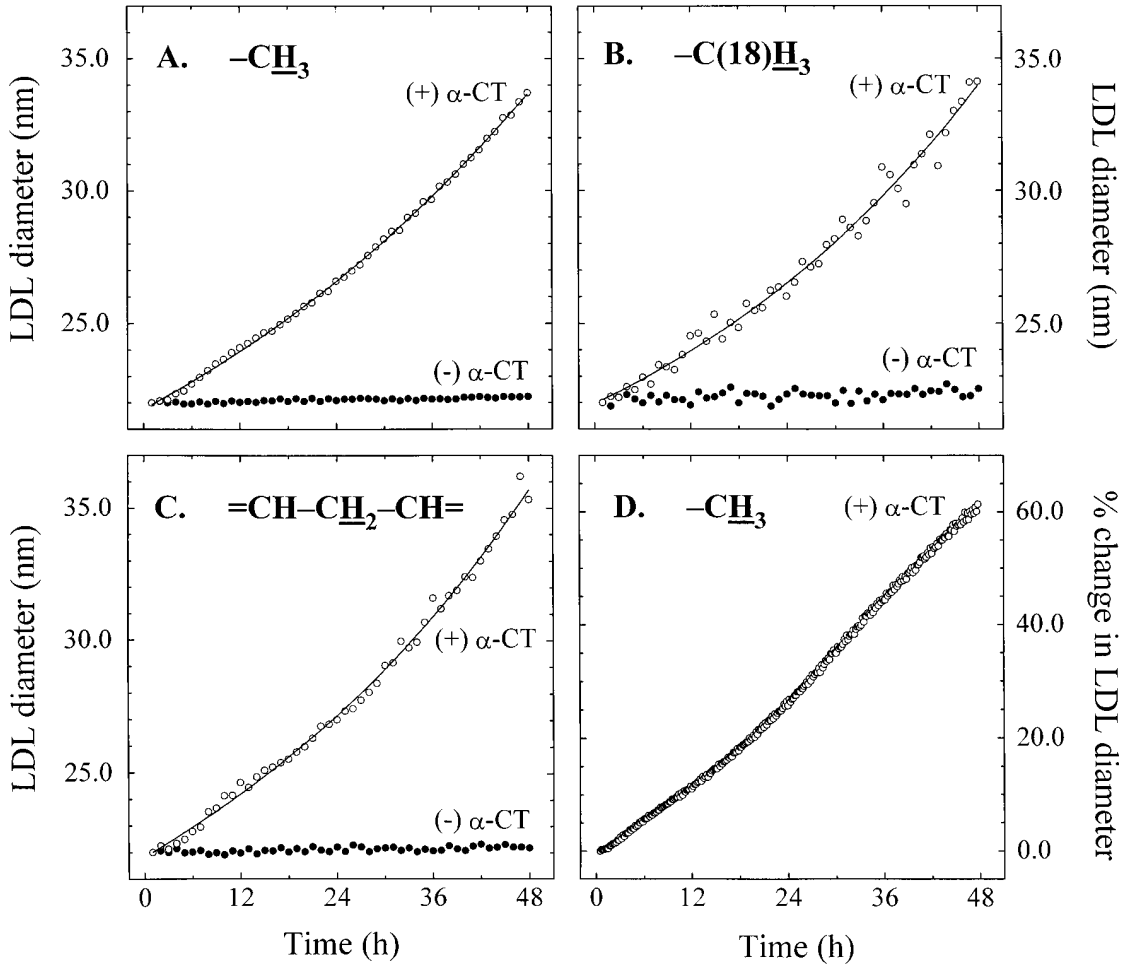

Fig. 2. Average particle size as a function of time in LDL incubated (at 37°C within the NMR spectrometer) in the presence ((+) α-CT) or absence ((-) α-CT) of α-chymotrypsin. The size changes have been calculated separately from the terminal methyl –C$\underline{H}_3$ (panel A), the cholesterol backbone –C(18)$\underline{H}_3$ (panel B), and the methylene =CH–C$\underline{H}_2$–CH= (panel C) ^{1}H NMR resonances by applying Eq. 1. The curves indicate fits of an exponential function to the data points. Panel D illustrates the percentage change in the average LDL particle diameter as a function of time, as calculated from the terminal methyl –C$\underline{H}_3$ resonance in another experiment, in which LDL was incubated in the presence of α-chymotrypsin and spectra were run every 10 min. Note that the signal-to-noise ratio was lower for the cholesterol backbone –C(18)$\underline{H}_3$ and the methylene =CH–C$\underline{H}_2$–CH= resonances than for the methyl –C$\underline{H}_3$ resonance (see Fig. 1), and thus the LDL diameters derived via their frequency shifts are slightly more scattered than those based on the –C$\underline{H}_3$ resonance.

tion. Another method, negative staining transmission electron microscopy, has shown that α-chymotrypsin treatment of LDL produces fused particles. A method based on fluorescence resonance energy transfer has specifically allowed us to follow LDL fusion even in LDL aggregates, but does not allow for detection of small changes or quantification of the changes in particle size (8).

In contrast, based on the modeling of the lipoprotein particle structure that has led to Eq. 1, ^{1}H NMR spectroscopy provides a direct method for the detection of fusion together with the possibility of quantifying the temporal changes in particle size. The current analysis, however, is not able to estimate the size distribution of the LDL particles in the sample containing a heterogeneous mixture of particles. Therefore, a full comparison with electron microscopic data on LDL particle size distributions is not possible. However, the diameter of 26.5 ± 0.6 nm (mean ± SD) obtained as an average value from the three analyzed ^{1}H NMR lipid resonances of LDL (Fig. 2, panels A–C), treated with α-chymotrypsin for 24 h, is in excellent agreement with the average particle diameter of 28.0 ± 7.8 nm from a negative staining electron microscopy analysis of LDL at the same time point of α-chymotrypsin-induced proteolysis (10). The other set of ^{1}H NMR data, for which the percentage change in LDL particle size (derived from the frequency shift behavior of the –C$\underline{H}_3$ resonance) as a function of time in the presence of α-chymotrypsin is shown in Fig. 2 (panel D), gave a value of 26.4 ± 1.2 nm at 24 h. Thus, the present results are in good general agreement with previous data on the effects of α-chymotrypsin treatment on LDL and show that the presented ^{1}H NMR methodology provides a unique and independent approach to study lipoprotein particle fusion. This quantitative comparison also suggests, perhaps slightly unexpectedly, that the structural changes taking place during the proteolytic process and LDL particle fusion seem to have

only minor effects on the quantitative applicability of the presented ^{1}H NMR methodology.

According to Eq. 1, only changes in the size of the individual lipoprotein particles, i.e., fusion, should change the frequencies of the ^{1}H NMR resonances of LDL lipids. In order to confirm this theoretical prediction and to further define the ^{1}H NMR spectroscopy characteristics of different kinds of LDL interactions, we also studied the interaction of LDL with anti-apoB-100 from sheep and from goat, dextran sulfate, and heparin, and compared the ^{1}H NMR spectroscopic information obtained with the electron microscopic characterization of the morphological details of these preparations.

Figure 3 shows the lipid fatty acid resonances in the aliphatic region of the ^{1}H NMR spectra from the LDL–sheep anti-apoB-100 complex (a), from fused LDL (treated with α-chymotrypsin for 48 h) (b), from the LDL–goat anti-apoB-100 complex (c), and from native LDL (d). Importantly, the frequency and shape of the resonances in the spectrum of the LDL–goat anti-apoB-100 complex and in the spectrum of native LDL are identical. In contrast, the spectrum of the LDL–sheep anti-apoB-100 complex shows drastic broadening of all the lipid resonances, resulting also in the disappearance of the cholesterol backbone –C(18)$\underline{H}_3$ peak at around 0.6 ppm. This is most likely an indication that the size of the LDL–goat anti-apoB-100 aggregates remained small enough to maintain rapid overall tumbling of the LDL particles but the LDL–sheep anti-apoB-100 aggregates grew large enough to significantly restrict the overall tumbling.

Figure 4 shows the electron microscopic characterization of the morphological details of the different LDL preparations, and provides an explanation for the ^{1}H NMR spectroscopic findings. In the LDL–goat anti-apoB-100 preparations (Fig. 4, panel C), distinct LDL particle aggregates with diameters of the order of a micrometer, and consisting of hundreds of individual particles, were generated. This is in contrast to the overall complexing and formation of huge LDL aggregates in the sheep anti-apoB-100-treated sample (Fig. 4, panel D). The electron microscopy also revealed that, despite the aggregation, the LDL particles retained their original size in the anti-apoB-100 preparations. Both the ^{1}H NMR spectroscopic and the electron microscopic characteristics of the LDL-dextran sulfate complexes closely resembled those of the LDL–sheep anti-apoB-100 aggregates, and the electrostatic interactions between LDL apoB-100 and the heparin molecules caused no ^{1}H NMR-detectable disturbances in the LDL lipid pool (data not shown).

The ^{1}H NMR experiments and the electron microscopic characterization together showed that limited aggregation of native-sized LDL particles in the LDL–goat anti-apoB-100 sample, without remarkable effects on their surface structures, i.e., on Δ or Δχ of the particles, did not lead to changes in the frequency of the lipid fatty acid resonances of LDL particles. This finding, and the experiments on the α-chymotrypsin-induced proteolytic fusion of LDL, confirmed the theoretical prediction that fusion has distinct characteristics in ^{1}H NMR spectrum. The experiments also clearly supported the usefulness of the physical lipoprotein particle model and the approximations necessary for the application of Eq. 1. The particle model should, in fact, be generally applicable for all lipoprotein particles (33). Therefore, the ^{1}H NMR methodol-

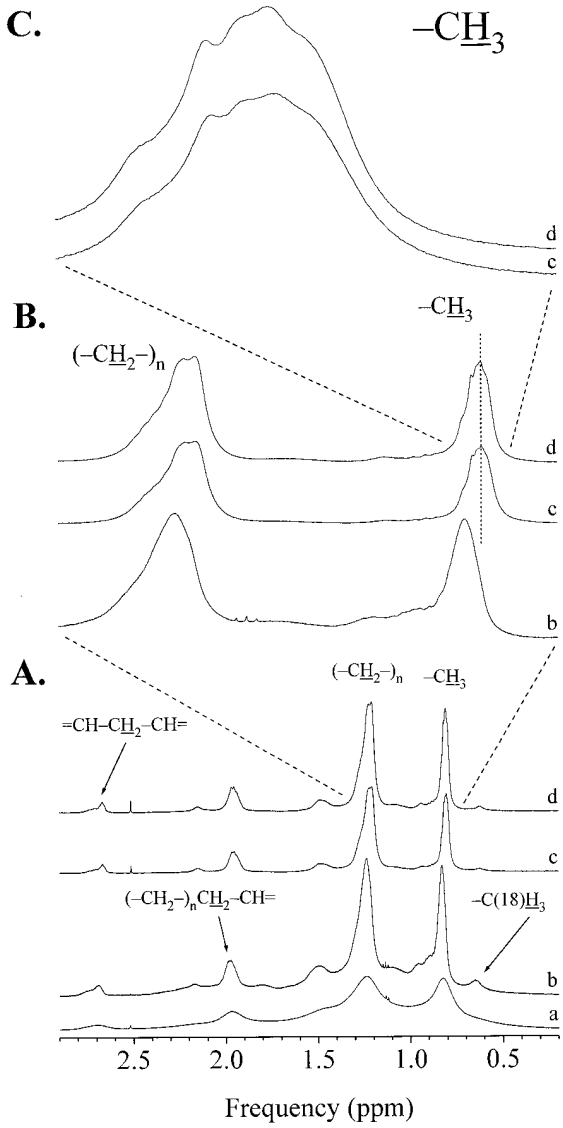

Fig. 3. The lipid fatty acid resonances in the aliphatic region of the ^{1}H NMR spectra from various LDL preparations are illustrated and assigned in panel A: an LDL–sheep anti-apoB-100 complex (a), fused LDL (treated with α-chymotrypsin for 48 h) (b), an LDL–goat anti-apoB complex (c), and native LDL (d). Underlining denotes the resonating proton for each peak; –C(18)$\underline{H}_3$ arises from the cholesterol backbones and the other resonances from the lipid fatty acid chains (24, 26). Panel B shows the methylene (–C$\underline{H}_2$–)$_n$ and methyl –C$\underline{H}_3$ resonances of the fused LDL (b), the LDL-goat anti-apoB complex (c), and native LDL (d). The dotted line at the terminal methyl –C$\underline{H}_3$ resonance position is to indicate the same resonance frequency in the spectrum of the LDL–goat anti-apoB complex (c) and of native LDL (d) and the difference between the frequency in the spectrum of the fused LDL (b). Panel C further emphasizes the close correspondence in the frequency position and also in the shape of the –C$\underline{H}_3$ resonance for the LDL–goat anti-apoB (c) and for native LDL (d) samples. All spectra shown are referenced to the external TSP reference at 0.0 ppm (for details, see Experimental Procedures).

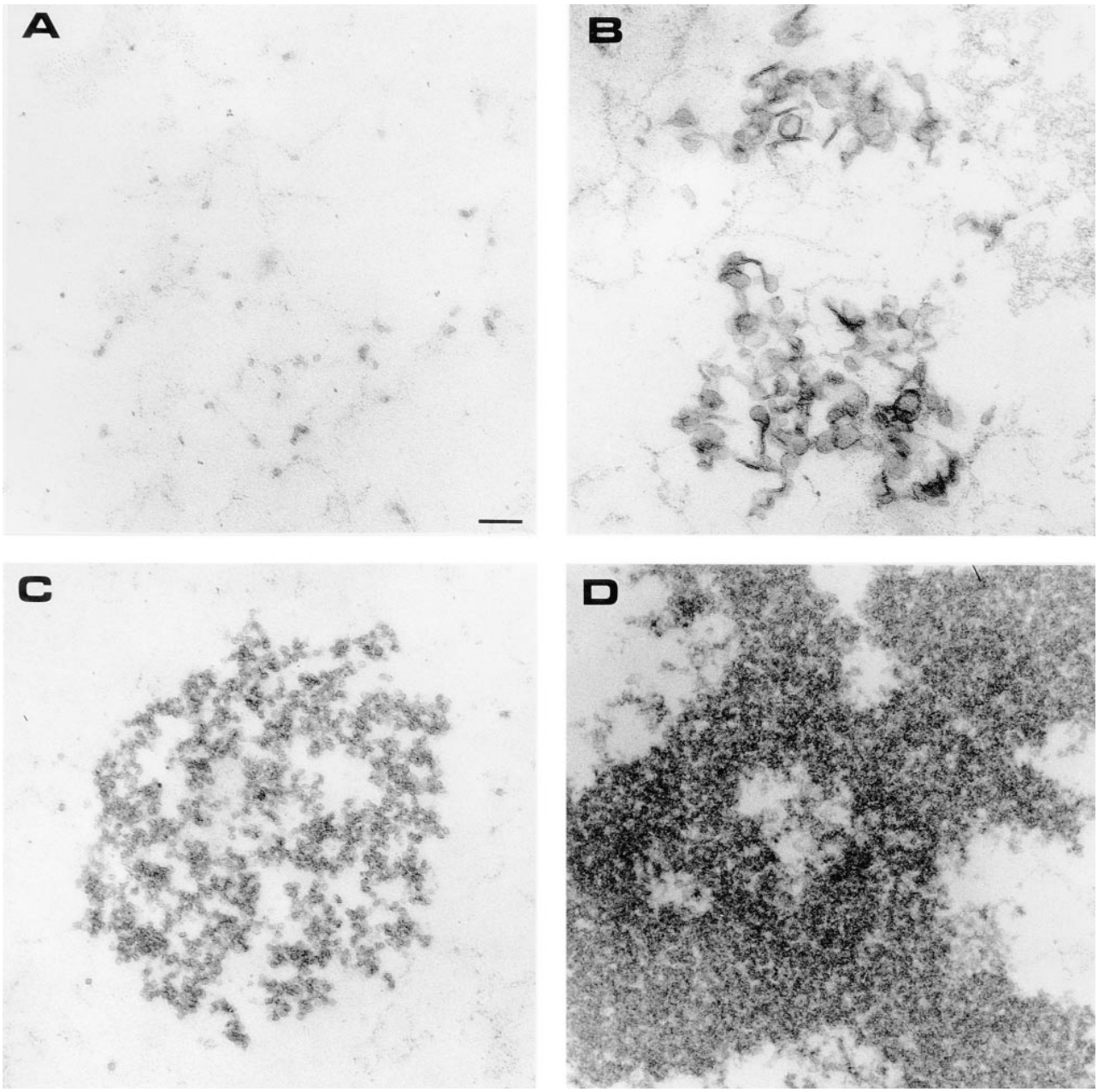

Fig. 4. Electron micrographs of native LDL (panel A), α-chymotrypsin-treated LDL (at 48 h) (panel B), LDL–goat anti-apoB-100 complex (panel C), and LDL–sheep anti-apoB-100 complex (panel D). Note the different sizes of the LDL aggregates in panels C and D and that, despite the aggregation, each LDL particle has retained its original size. Bar = 100 nm.

ogy presented here need not be limited to studies of LDL particle fusion but should also be applicable to the study of lipoprotein particle interactions in general.

This study was focused on the phenomenological aspects of proteolytic LDL fusion and presents a methodological basis for kinetic in vitro studies of lipoprotein particle modifications, making it possible to distinguish, follow up, and quantify subsequent particle fusion. It should also be remembered that, in addition to supplying direct data on particle fusion, ^{1}H NMR spectroscopy can provide a wealth of physico–chemical information on lipoprotein lipids (24–31). Comprehensive analysis of these complex overlapping data is tedious, requiring sophisticated mathematical methods and software. This is currently not fully established, but it is likely that recent advances in spectral analysis (24, 38) will enable such an analysis to be performed. Steps aimed toward full utilization of the physico–chemical lipoprotein lipid information provided by ^{1}H NMR spectroscopy are currently underway in our laboratory. Moreover, the good resolution in the ^{1}H NMR spectra of the LDL–goat anti-apoB-100 aggregates and in the case of the LDL–heparin interactions suggest that the ^{1}H NMR methodology introduced here may also allow studies of the fate of LDL particles in other in vitro models that mimic the extracellular LDL interactions in vivo.

The authors thank Katariina Öörni for stimulating discussions and Päivi Hiironen for excellent technical assistance. Financial support from the Academy of Finland to MAK and from the Tauno Tönninki Foundation to AK is also gratefully acknowledged.

Manuscript received 29 December 1997 and in revised form 23 April 1998.

REFERENCES

1. Pasquinelli, G., P. Preda, M. Vici, M. Gargiulo, A. Stella, M. D'Addato, and R. Laschi. 1989. Electron microscopy of lipid deposits in human atherosclerosis. *Scanning Microsc.* **3:** 1151–1159.
2. Tirziu, D., A. Dobrian, C. Tasca, M. Simionescu, and N. Simionescu. 1995. Intimal thickenings of human aorta contain modified reassembled lipoproteins. *Atherosclerosis.* **112:** 101–114.
3. Nievelstein, P. F. E. M., A. M. Fogelman, G. Mottino, and J. S. Frank. 1991. Lipid accumulation in rabbit aortic intima 2 hours after bolus infusion of low density lipoprotein. A deep-etch and immunolocalization study of ultrarapidly frozen tissue. *Arterioscler. Thromb.* **11:** 1795–1805.
4. Bocan, T. M., T. A. Schifani, and J. R. Guyton. 1986. Ultrastructure of the human aortic fibrolipid lesion. Formation of the atherosclerotic lipid-rich core. *Am. J. Pathol.* **123:** 413–424.
5. Williams, K. J. and I. Tabas. 1995. The response-to-retention hypothesis of early atherogenesis. *Arterioscler. Thromb. Vasc. Biol.* **15:** 551–561.
6. Guyton, J. R., and K. F. Klemp. 1996. Development of the lipid-rich core in human atherosclerosis. *Arterioscler. Thromb. Vasc. Biol.* **16:** 4–11.
7. Kruth, H. S. 1997. The fate of lipoprotein cholesterol entering the arterial wall. *Curr. Opin. Lipidol.* **8:** 246–252.
8. Pentikäinen, M. O., E. M. P. Lehtonen, K. Öörni, S. Lusa, P. Somerharju, M. Jauhiainen, and P. T. Kovanen. 1997. Human arterial proteoglycans increase the rate of proteolytic fusion of low density lipoprotein particles. *J. Biol. Chem.* **272:** 25283–25288.
9. Kokkonen, J. O., and P. T. Kovanen. 1989. Proteolytic enzymes of mast cell granules degrade low density lipoproteins and promote their granule-mediated uptake by macrophages in vitro. *J. Biol. Chem.* **264:** 10749–10755.
10. Piha, M., L. Lindstedt, and P. T. Kovanen. 1995. Fusion of proteolyzed LDL in the fluid phase: a novel mechanism generating atherogenic lipoprotein particles. *Biochemistry.* **34:** 10120–10129.
11. Paananen, K., and P. T. Kovanen. 1994. Proteolysis and fusion of low density lipoprotein particles independently strengthen their binding to exocytosed mast cell granules, *J. Biol. Chem.* **269:** 2023–2031.
12. Paananen, K., J. Saarinen, A. Annila, and P. T. Kovanen. 1995. Proteolysis and fusion of low density lipoprotein particles strengthen their binding to human aortic proteoglycans, *J. Biol. Chem.* **270:** 12257–12262.
13. Xu, X. X., and I. Tabas. 1991. Sphingomyelinase enhances low density lipoprotein uptake and ability to induce cholesteryl ester accumulation in macrophages. *J. Biol. Chem.* **266:** 24849–24858.
14. Schissel, S. L., J. Tweedie-Hardman, J. H. Rapp, G. Graham, K. J. Williams, and I. Tabas. 1996. Rabbit aorta and human atherosclerotic lesions hydrolyze the sphingomyelin of retained low-density lipoprotein: proposed role for arterial-wall sphingomyelinase in subendothelial retention and aggregation of atherogenic lipoproteins. *J. Clin. Invest.* **98:** 1455–1464.
15. Öörni, K., J. K. Hakala, A. Annila, and P. T. Kovanen. 1997. Modification of low density lipoprotein with phospholipase A_2 generates aggregated and fused particles with increased strength of binding to proteoglycans. *Atherosclerosis.* **134:** 225–226. Abstract.
16. Khoo, J. C., E. Miller, P. McLoughlin, and D. Steinberg. 1988. Enhanced macrophage uptake of low density lipoprotein after self-aggregation. *Arteriosclerosis.* **8:** 348–358.
17. Guyton, J. R., K. F. Klemp, and M. P. Mims. 1991. Altered ultrastructural morphology of self-aggregated low density lipoproteins: coalescence of lipid domains forming droplets and vesicles. *J. Lipid Res.* **32:** 953–962.
18. Dobrian, A., R. Mora, M. Simionescu, and N. Simionescu. 1993. In vitro formation of oxidatively modified and reassembled human low-density lipoproteins: antioxidant effect of albumin. *Biochim. Biophys. Acta.* **1169:** 12–24.
19. Chao, F. F., E. J. Blanchette-Mackie, V. V. Tertov, S. I. Skarlatos, Y. J. Chen, and H. S. Kruth. 1992. Hydrolysis of cholesteryl ester in low density lipoprotein converts this lipoprotein to a liposome. *J. Biol. Chem.* **267:** 4992–4998.
20. Pentikäinen, M. O., E. M. P. Lehtonen, and P. T. Kovanen. 1996. Aggregation and fusion of modified low density lipoprotein. *J. Lipid Res.* **37:** 2638–2649.
21. Bell, J. D., P. J. Sadler, A. F. Macleod, P. R. Turner, and A. La Ville. 1987. ^{1}H NMR studies of human blood plasma. Assignment of resonances for lipoproteins. *FEBS Lett.* **219:** 239–243.
22. Otvos, J. D., E. J. Jeyarajah, D. W. Bennett, and R. M. Krauss. 1992. Development of a proton nuclear magnetic resonance spectroscopic method for determining plasma lipoprotein concentrations and subspecies distributions from a single, rapid measurement. *Clin. Chem.* **38:** 1632–1638.
23. Ala-Korpela, M., A. Korhonen, J. Keisala, S. Hörkkö, P. Korpi, L. P. Ingman, J. Jokisaari, M. J. Savolainen, and Y. A. Kesäniemi. 1994. ^{1}H NMR based quantitation of human lipoproteins and their lipid contents directly from plasma. *J. Lipid Res.* **35:** 2292–2304.
24. Ala-Korpela, M. 1995. ^{1}H NMR spectroscopy of human blood plasma. *Prog. Nucl. Magn. Reson. Spectr.* **27:** 475–554.
25. Lodge, J. K., P. J. Sadler, M. L. Kus, and P. G. Winyard. 1995. Copper-induced LDL peroxidation investigated by ^{1}H-NMR spectroscopy. *Biochim. Biophys. Acta.* **1256:** 130–140.
26. Nicholson, J. K., P. J. D. Foxall, M. Spraul, R. D. Farrant, and J. C. Lindon. 1995. 750 MHz ^{1}H and ^{1}H-^{13}C NMR spectroscopy of human blood plasma. *Anal. Chem.* **67:** 793–811.
27. Bell, J. D., M. L. Barnard, H. G. Parkes, E. L. Thomas, C. H. Brennan, S. C. Cunnane, and P. C. Dagnelie. 1996. Effects of n–3 fatty acids on the NMR profile of plasma lipoproteins. *J. Lipid Res.* **37:** 1664–1674.
28. Parks J. S., and H. Hauser. 1996. Low density lipoprotein particle size and core cholesteryl ester physical state affect the proton NMR magnetic environment of fatty acid methylene and methyl nuclei. *J. Lipid Res.* **37:** 1289–1297.
29. Murphy, H. C., M. Ala-Korpela, J. J. White, A. Raoof, J. D. Bell, M. L. Barnard, S. P. Burns, and R. A. Iles. 1997. Evidence for distinct behaviour of phosphatidylcholine and sphingomyelin at the low density lipoprotein surface. *Biochem. Biophys. Res. Commun.* **234:** 733–737.
30. Ala-Korpela, M., A. Korhonen, M. J. Liinamaa, M. J. Savolainen, J. Jokisaari, and Y. A. Kesäniemi. 1997. ^{1}H NMR and prior knowledge based lineshape fitting analysis: a powerful combination for quantitative biochemistry of plasma and lipoproteins. *J. Magn. Reson. Anal.* **3:** 15–20.
31. Korhonen, A., M. Ala-Korpela, M. J. Liinamaa, J. Jokisaari, Y. A. Kesäniemi, and M. J. Savolainen. 1997. Assessment of cholesteryl ester transfer protein function in lipoprotein mixtures by ^{1}H NMR spectroscopy. *NMR Biomed.* **10:** 303–308.
32. Hiltunen, Y., M. Ala-Korpela, J. Jokisaari, S. Eskelinen, K. Kiviniitty, M. Savolainen, and Y. A. Kesäniemi. 1991. A lineshape fitting model for ^{1}H NMR spectra of human blood plasma. *Magn. Reson. Med.* **21:** 222–232.
33. Lounila, J., M. Ala-Korpela, J. Jokisaari, M. J. Savolainen, and Y. A. Kesäniemi. 1994. Effects of orientational order and particle size on the NMR line positions of lipoproteins. *Phys. Rev. Lett.* **72:** 4049–4052.
34. Havel, R. J., H. A. Eder, and J. H. Bragdon. 1955. The distribution and chemical composition of ultracentrifugally separated lipoproteins in human serum. *J. Clin. Invest.* **34:** 1345–1353.
35. Lowry, O. H., N. J. Rosebrough, A. L. Farr, and R. J. Randall. 1951. Protein measurement with the Folin phenol reagent. *J. Biol. Chem.* **193:** 265–275.
36. Camejo, G., G. Fager, B. Rosengren, E. Hurt-Camejo, and G. Bondjers. 1993. Binding of low density lipoproteins by proteoglycans synthesized by proliferating and quiescent human arterial smooth muscle cells. *J. Biol. Chem.* **268:** 14131–14137.
37. Hwang, T-L., and A. J. Shaka. 1995. Water suppression that works—excitation sculpting using arbitrary wave-forms and pulsed-field gradients. *J. Magn. Reson.* **112A:** 275–279.
38. Laatikainen, R., M. Niemitz, W. J. Malaisse, M. Biesemans, and R. Willem. 1996. A computational strategy for the deconvolution of NMR-spectra with multiplet structures and constraints—analysis of overlapping C–13–H–2 multiplets of C–13 enriched metabolites from cell-suspensions incubated in deuterated media. *Magn. Reson. Med.* **36:** 359–365.